

Traveling capillary waves on the boundary of a disc

Sergey A. Dyachenko[†]

Department of Applied Mathematics, University of Washington
Seattle, WA 98195 USA

(Received xx; revised xx; accepted xx)

We find a new class of solutions that are traveling waves on the boundary of two-dimensional droplet of ideal fluid. We assume that the free surface is subject only to the force of surface tension, and the fluid flow is potential. We use the canonical Hamiltonian variables discovered in the work Zakharov (1968), and conformally map lower complex plane to the interior of a fluid droplet. We write the equations in the form originally discovered in Dyachenko (2001) for infinitely deep water, and adapted to bounded fluid in the work Dyachenko (2019). The new class of solutions satisfies a pseudodifferential equation which is similar to the Babenko equation for the Stokes wave.

1. Introduction

A free surface of ideal fluid is a classical and fundamental problem in theoretical physics. The motion of the free surface of ocean has been extensively studied, but as of yet there are fundamental questions that await to be addressed, such as: how do the deep water waves break, and is 2D potential flow with free surface an integrable system? In some approximations of Euler equations, one may obtain well-known physical systems that are integrable, namely the Korteweg–de–Vries equation, or the famous nonlinear Schrödinger equation. As for the primordial Euler equations, the question of integrability remains elusive. In the recent years, there has been some development in this field, and the work Dyachenko *et al.* (2019) shows that new previously unknown nontrivial integrals of motion associated with 2D inviscid potential flow exist.

The study of free surface flows has a long history, and the modern view of the field may be traced to the works of Dirichlet (1860), and Stokes (1880). In the year 1957, Crapper (1957) discovered traveling capillary waves over infinite depth fluid by means of hodograph transformation, and almost twenty years after, Kinnersley (1976) found exact solutions for traveling waves on fluid flow in finite depth. The works Crowdy (1999*a*) and Crowdy (1999*b*) have found solutions of the free boundary problem by prescribing a specific singularities of the flow potential. For generic potential flow Zakharov (1968) discovered that the motion of the boundary and the velocity of the fluid is described only in terms of the surface potential, and surface elevation which are the canonical Hamiltonian variables of this system. In the works Dyachenko *et al.* (1996*a*), Dyachenko *et al.* (1996*b*) the Hamiltonian formalism in the physical variables was used to find the equations of motion in conformal variables. The conformal variables allow for a much richer geometry of the free surface since it is now represented in parametric form, moreover conformal variables allow a simple and exact calculation of the Dirichlet–to–Neumann operator. In Dyachenko (2001), a new set of variables that are suitable for both theoretical and numerical simulations have been presented. In the recent work Dyachenko (2019), the

[†] Email address for correspondence: sergd@uw.edu

conformal variables approach has been extended from a problem posed on an infinite free boundary of surface of ocean, to a bounded surface that encloses a finite volume droplet of water.

The purpose of the present paper is to use the formulation developed in the previous work Dyachenko (2019) to demonstrate a new class of solutions to the free boundary problem on a droplet. These solutions have a very simple motion: the shape of the free boundary rotates around the center of mass at a constant angular velocity. The resulting equation is pseudodifferential and is similar to the Babenko (1987) for the Stokes waves – the progressive gravity waves on the surface of infinite ocean. Large amplitude solutions of the presented equation are the subject of ongoing work, however the small amplitude linear waves on the boundary of a disc of fluid are discussed, and their dispersion relation is obtained. We illustrate with the results of numerical simulations of the full dynamical equations, and demonstrate excellent agreement with the theoretical predictions. The standard dispersion of capillary waves around flat water may be obtained as a short wavelength limit of the dispersion waves on a disc.

The present work is a precursor to the study of fully nonlinear solutions of the traveling wave equation. Of a particular interest is the nature of limiting traveling wave that is conjectured to exist in the presented equation.

2. Formulation of the Problem

We study the motion of ideal fluid in 2D assuming that fluid flow is potential, i.e. the fluid velocity is $\nabla\varphi(\mathbf{r}, t)$. We note that this classical problem is Hamiltonian, which is given by the formula:

$$H = \frac{1}{2} \iint_D (\nabla\varphi)^2 dx dy + \sigma \int_{\partial D} dl, \quad (2.1)$$

where ∇ denotes the gradient operator, σ is the surface tension coefficient, and D is the fluid domain, which is assumed to be bounded and the boundary, ∂D , is a closed curve in 2D, with dl being the elementary arclength along ∂D . It is evident that a stationary fluid disc is a global minimum of the potential energy subject to fixed fluid mass, μ , defined as follows:

$$\mu = \iint_D dx dy. \quad (2.2)$$

In the same manner as water waves are studied on the surface of deep water, the question of the surface waves travelling on the boundary of a fluid disc may be posed.

It is natural to choose inertial reference frame in which $z = x + iy = 0$ is the coordinate of the center of mass of fluid. The center of mass is stationary in our chosen reference frame, hence the total momentum, \mathcal{P} , is zero:

$$\mathcal{P} = \mathcal{P}_x + i\mathcal{P}_y = \iint_D (\varphi_x + i\varphi_y) dx dy \quad (2.3)$$

Moreover, the angular momentum, \mathcal{J} of the fluid droplet may also be found from the formula:

$$\mathcal{J} = \iint_D [\mathbf{r} \times \nabla\varphi] dx dy \quad (2.4)$$

and is a constant of motion.

3. Mechanics of droplet and the conformal map

We introduce a time-dependent conformal map $z(w, t)$ that maps a semi-infinite periodic dimensionless strip $w = u + iv \in \{-\pi \leq u < \pi, v \leq 0\}$ to the physical fluid domain, $x + iy \in D$. The specification of the conformal is incomplete unless the mapping of one extra point in the fluid is also fixed, we will require that $z(w \rightarrow -i\infty) = z_0$. The choice $z_0 = 0$ is almost always the most convenient one, however by no means it is a unique choice. The constants of motion are conveniently expressed in terms of the boundary value of the velocity potential, and the conformal map.

3.1. The Hamiltonian, fluid mass and total momentum

We may transform Hamiltonian, H , from the physical plane to the conformal domain in the same manner as it has been done in the work (Dyachenko *et al.* (1996a)) and is given by:

$$\mathcal{H} = \frac{1}{2} \iint_D (\nabla\varphi)^2 dx dy + \sigma \int_{\partial D} dl = \frac{1}{2} \int_{-\pi}^{\pi} \psi \hat{k} \psi du + \sigma \int_{-\pi}^{\pi} |z_u| du \quad (3.1)$$

where $\hat{k} = -\hat{H}\partial_u$ and \hat{H} is the Hilbert transform, and $\psi(u, t) = \varphi(x(u, t), y(u, t), t)$ is the value of the velocity potential on the free-surface.

The total volume of an incompressible fluid is proportional to the total mass of the fluid, μ , which is a trivial motion constant. The fluid volume and the total momentum are given by the formulas:

$$\mu = \iint_D dx dy = \frac{1}{2} \iint (\nabla \cdot \mathbf{r}) dx dy = \frac{1}{4i} \int [z\bar{z}_u - \bar{z}z_u] du \quad (3.2)$$

$$\mathcal{P}_x + i\mathcal{P}_y = \iint_D \nabla\varphi dx dy = i \int \psi z_u du, \quad (3.3)$$

where $\mathbf{r} = (x, y)^T$.

3.2. The Angular Momentum

The angular momentum of the fluid, \mathcal{J} , is another motion constant. We may write it in the physical plane as follows:

$$\mathcal{J} = \iint [\mathbf{r} \times \nabla\phi] dx dy = \iint (x\phi_y - y\phi_x) dx dy, \quad (3.4)$$

and after integration by parts, it reduces to a surface integral:

$$\mathcal{J} = -\frac{1}{2} \iint (\nabla(r^2) \cdot \nabla\theta) dx dy = -\frac{1}{2} \int r^2 \frac{\partial\theta}{\partial \mathbf{n}} dl, \quad (3.5)$$

where $r = \sqrt{x^2 + y^2}$ and \mathbf{n} is the unit normal to the free surface. In the conformal variables the angular momentum is given by the following equation:

$$\mathcal{J} = -\frac{1}{2} \int |z|^2 \psi_u du, \quad \frac{d\mathcal{J}}{dt} = 0. \quad (3.6)$$

Although moment of inertia is not a constant in a generic time-dependent flow, it is convenient to consider when the fluid rotates without changing the shape of its surface.

The moment of inertia, \mathcal{I} , is introduced as follows:

$$\mathcal{I} = \iint r^2 dx dy = \frac{1}{4} \iint (\nabla r^2 \cdot \nabla r^2) dx dy = \frac{1}{8} \int |z|^2 \partial_v |z|^2 du.$$

However, $|z|^2$ is not analytic, and therefore one cannot use the Hilbert transform to relate the derivatives in u and v . As a result the moment of inertia is written in the following form:

$$\mathcal{I} = \frac{1}{8i} \int |z|^2 (z \bar{z}_u - \bar{z} z_u) du. \quad (3.7)$$

We note that the moment of inertia satisfies an ordinary differential equation:

$$\frac{d\mathcal{I}}{dt} = \int |z|^2 \hat{k} \psi du. \quad (3.8)$$

In the section 5, we seek such flows that the geometry of the droplet is preserved, and hence the moment of inertia is fixed. The time-derivative vanishes for such fluid flow.

3.3. The Center of Mass

The center of mass of the fluid is located at the origin, and in conformal variables it may also be determined from integrating vector $\mathbf{r} = (x, y)^T$ over the fluid domain, namely

$$\mathbf{R}_{cm} = \iint_D \mathbf{r} dx dy = \frac{1}{2} \iint \nabla (r^2) dx dy = \frac{1}{2} \int r^2 d\mathbf{l}, \quad (3.9)$$

and in the conformal plane, this expression becomes:

$$\mathbf{R}_{cm} = \frac{i}{2} \int |z|^2 z_u du. \quad (3.10)$$

When the conformal map, $z(w)$, is written as a Fourier series, the constant term, z_0 is recovered from the relation:

$$2iz_0 = \frac{1}{\mu} \int |z - z_0|^2 z_u du, \quad (3.11)$$

that is derived from (3.10). The motion of the center of mass is subject to a trivial ODE:

$$\mu \frac{d\mathbf{R}_{cm}}{dt} = \mathbf{P}. \quad (3.12)$$

and as mentioned before, $\mathbf{R}_{cm} = 0$ for all time when total momentum $\mathbf{P} = 0$.

4. The Complex Equations of Motion

We use the variational approach to write the equations of motion in complex variables, but they may also be obtained directly from the Bernoulli equation and the kinematic condition in physical variables (see also Dyachenko (2019)):

$$\left. \frac{\partial F}{\partial t} + (\nabla \varphi \cdot \nabla F) \right|_{F=0} = 0, \quad (4.1)$$

$$\left. \frac{\partial \varphi}{\partial t} \right|_{F=0} + \left. \frac{|\nabla \varphi|^2}{2} \right|_{F=0} + \sigma \kappa = 0, \quad (4.2)$$

where $F(x, y, t)$ is the implicit form of the free surface, and κ is the local curvature. The Lagrangian, \mathcal{L} , is formed from the Hamiltonian, H , while noting that in the physical plane the surface potential and elevation are canonical variables as first discovered in the work Zakharov (1968):

$$\mathcal{L} = \frac{1}{2i} \int \psi (z_t \bar{z}_u - \bar{z}_t z_u) - \mathcal{H} + i \int f \left(\hat{P}^+ z_u - \hat{P} \bar{z}_u \right) \quad (4.3)$$

in terms of the real and imaginary parts of z it can also be written as follows:

$$\mathcal{L} = \int \psi (y_t x_u - y_u x_t) du - \int f (y_u + \hat{k}x) du - \mathcal{H}, \quad (4.4)$$

where $f(u, t)$ is the Lagrange multiplier enforcing the Cauchy–Riemann conditions on the components of $z(w, t)$. We form action, \mathcal{S} , as follows:

$$\mathcal{S} = \int \mathcal{L} dt, \quad \text{and} \quad \frac{\delta \mathcal{S}}{\delta \psi} = 0, \quad \frac{\delta \mathcal{S}}{\delta f} = 0, \quad \frac{\delta \mathcal{S}}{\delta x} = 0, \quad \frac{\delta \mathcal{S}}{\delta y} = 0. \quad (4.5)$$

and derive kinematic and dynamic equations from the least action principle.

4.1. Kinematic Equation

The implicit form of the kinematic equation for the conformal map is given by:

$$z_t \bar{z}_u - \bar{z}_t z_u = \bar{\Phi}_u - \Phi_u, \quad (4.6)$$

or in terms of the real and imaginary parts of z it yields:

$$y_t x_u - y_u x_t = \hat{k} \psi. \quad (4.7)$$

In general, the conformal map, z can be expanded in Fourier series as follows:

$$z(u, t) = z_0(t) + z_{-1}(t)e^{-iu} + \dots, \quad (4.8)$$

and similarly, $z_t(u, t)$. The conformal mapping $z(w, t)$ is not fully specified yet, and one extra condition on the mapping of the point at infinity may still be enforced. For instance, one may check that a stationary solution, a unit disc, may be written as a one-parameter family of conformal maps:

$$z(w) = e^{-iw} \frac{1 + \bar{A}e^{iw}}{1 + Ae^{-iw}}, \quad (4.9)$$

where A is a free complex parameter with $|A| < 1$. It is convenient to set the image of $w \rightarrow -i\infty$ to be the center of mass of fluid at every instant of time, then:

$$z(w \rightarrow -i\infty) = 0 \quad \text{and} \quad z_t(w \rightarrow -i\infty) = 0, \quad (4.10)$$

which is the natural choice, but it is not unique. Although the value of $z_0(t)$ does not contribute to the dynamics of droplet, its time-derivative does. For convenience we will denote:

$$z_t(w \rightarrow -i\infty) = \frac{dz_0}{dt} = i\bar{v}_0(t). \quad (4.11)$$

With the aforementioned choice of $v_0(t) = 0$. Another choice is:

$$v_0 = i\langle R\Phi_u \rangle \quad \text{and} \quad z_0 = \xi, \quad (4.12)$$

where $Rz_u = 1$ and $|\xi| \in D$, and angular brackets denote average value over one period. With the latter choice, the point at infinity travels with fluid particle originated at $z_0 = \xi$ at time $t = 0$.

We define the complex transport velocity, U :

$$U = \hat{P} \left[\frac{i(\Phi_u - \bar{v}_0 z_u) + c.c.}{|z_u|^2} \right], \quad (4.13)$$

where $2\hat{P} = 1 + i\hat{H}$ is the projection operator. The kinematic condition can now be resolved for time-derivative and yields:

$$\frac{z_t}{z_u} - \frac{i\bar{v}_0}{z_u} = iU, \quad \text{or} \quad z_t = i\bar{v}_0 + iU z_u \quad (4.14)$$

The last formula gives a clear interpretation of the time-evolution of the conformal map due to motion of the point at $v \rightarrow -\infty$, and the relative motion of the fluid given by $iU z_u$ which does not contain a constant term in its Fourier series.

4.2. Dynamic Condition

Variation of action in \bar{z} results in the following implicit relations for the surface potential:

$$\psi_t z_u - \psi_u z_t + i\sigma \partial_u \left(\frac{z_u}{|z_u|} \right) = (1 - i\hat{H}) f_u \quad (4.15)$$

and by extracting the real and imaginary part one finds that:

$$\psi_t x_u - \psi_u x_t - \sigma \partial_u \left(\frac{y_u}{|z_u|} \right) = f_u, \quad (4.16)$$

$$\psi_t y_u - \psi_u y_t + \sigma \partial_u \left(\frac{x_u}{|z_u|} \right) = \hat{k} f. \quad (4.17)$$

These equations can be solved for the Lagrange multiplier, Λ_u , to find:

$$\Lambda_u = f_u + i\hat{H} f_u = -\frac{\Phi_u^2}{2z_u}. \quad (4.18)$$

The implicit form of the dynamic condition becomes:

$$\psi_t \bar{z}_u - \psi_u \bar{z}_t + \frac{\Phi_u^2}{2z_u} = i\sigma \partial_u \left(\frac{\bar{z}_u}{|z_u|} \right), \quad (4.19)$$

and the Bernoulli equation is found:

$$\left(\Phi_t - \Phi_u \frac{z_t}{z_u} \right) + \left(\bar{\Phi}_t - \bar{\Phi}_u \frac{\bar{z}_t}{\bar{z}_u} \right) + \left| \frac{\Phi_u}{z_u} \right|^2 + i\sigma \frac{\bar{z}_u z_{uu} - z_u \bar{z}_{uu}}{|z_u|^3} = 0. \quad (4.20)$$

Note, that the last term is simply the local curvature of the free surface. We apply projection operator, \hat{P} , and obtain explicit equation of motion for the complex potential. We define auxiliary analytic function B as follows:

$$B = \hat{P} \left[\frac{|\Phi_u|^2}{|z_u|^2} + i\sigma \frac{\bar{z}_u z_{uu} - z_u \bar{z}_{uu}}{|z_u|^3} \right], \quad (4.21)$$

and

$$\Phi_t - \Phi_u \frac{z_t}{z_u} + B = 0. \quad (4.22)$$

We substitute the equation (4.14) into (4.20) and write the full system of hydrodynamic

equations:

$$z_t - i\bar{v}_0 = iUz_u, \quad (4.23)$$

$$\Phi_t - \bar{v}_0 \frac{i\Phi_u}{z_u} = iU\Phi_u - B \quad (4.24)$$

The equations are now recast in standard R and V variables, that have been discovered by A. I. Dyachenko Dyachenko (2001):

$$R = \frac{1}{z_u}, \quad V = \frac{i\Phi_u}{z_u}, \quad (4.25)$$

and gives:

$$R_t = i[UR_u - U_uR], \quad (4.26)$$

$$V_t = i[(U + \bar{v}_0R)V_u - B_uR], \quad (4.27)$$

and the auxiliary analytic functions are:

$$U = \hat{P}[(V - v_0)\bar{R} + (\bar{V} - \bar{v}_0)R], \quad (4.28)$$

$$B = \hat{P}[|V|^2 + 2\sigma|Q|^2 + 2i\sigma(Q\bar{Q}_u - \bar{Q}Q_u)], \quad (4.29)$$

where $Q = \sqrt{Re^{-iu}}$. With the natural choice, $z_t(w \rightarrow -i\infty) \rightarrow 0$, one recovers the equations in standard R, V variables with $v_0 = 0$. The explicit equations for R and V are convenient for numerical simulation of the free surface of a droplet of ideal fluid.

5. Travelling waves on a disk

The conformal map that describes a wave traveling on the free surface of a disc, and the corresponding complex potential that is found from the kinematic condition (4.7) are given by:

$$z(u, t) = e^{-i\Omega t} z(u - \Omega t) \quad \text{and} \quad \Phi(u, t) = i\Omega \hat{P}|z|^2 - \beta t \quad (5.1)$$

where β is the Bernoulli constant. We note that the equations of motion are invariant under the change of variables $u \rightarrow u - \Omega t$, and thus the solution may be sought in the form $z = z(u)$. In such a case the time-derivatives of z and $\psi = Re\Phi$ are given by the following relations:

$$\psi_t = -\beta \quad \text{and} \quad z_t = -i\Omega z. \quad (5.2)$$

After substitution in the equations (4.16) and (4.17) we find that a traveling wave satisfies the real equation:

$$2\beta y_u - \frac{\Omega^2}{2} [x\hat{k}|z|^2 - \hat{H}(y\hat{k}|z|^2)] - \sigma \partial_u \left[\frac{x_u}{|z_u|} - \hat{H} \left(\frac{y_u}{|z_u|} \right) \right] = 0 \quad (5.3)$$

or, alternatively, it may be formulated in complex form:

$$2i\beta z_u + \Omega^2 \hat{P} [z\hat{k}|z|^2] + 2\sigma \partial_u \hat{P} \left[\frac{z_u}{|z_u|} \right] = 0, \quad (5.4)$$

and the Bernoulli constant may be obtained from multiplication of the equation (5.4) by \bar{z} and integrating over the period:

$$\mu\beta = \Omega \mathcal{J} + \frac{\sigma}{2} \langle |z_u| \rangle, \quad (5.5)$$

where the angular brackets denote integral over one period.

5.1. Variational approach to traveling waves

The traveling wave solution may be obtained directly from variational approach. We consider Hamiltonian, \mathcal{H} , in the inertial reference frame given as the sum of kinetic and potential energy:

$$\mathcal{H} = \frac{\Omega^2}{8} \int |z|^2 \hat{k} |z|^2 du + \sigma \int |z_u| du. \quad (5.6)$$

In a (non-inertial) reference frame where the shape of the surface does not change, the Hamiltonian, \mathcal{H}' is modified by a contribution from the angular momentum Landau & Lifshitz (1976):

$$\mathcal{H}' = \mathcal{H} + \mathcal{J}\Omega. \quad (5.7)$$

where \mathcal{J} is defined in the equation (3.6). The equation describing a traveling wave may also be recovered from variation of the Hamiltonian (5.7), while holding the fluid mass, \mathcal{M} , fixed and enforcing that $z(u)$ is the boundary value of analytic function via Lagrange multiplier:

$$\delta \left(\mathcal{H}' - \lambda \mathcal{M} - \int f \left(\hat{P}^+ z_u + c.c. \right) du \right) = 0 \quad (5.8)$$

where $2\hat{P}^+ = 1 - i\hat{H}$. The constant, λ , and the function, $f(u)$, are the Lagrange multipliers. The angular momentum defined in (3.6) for the traveling wave acquires a simple form:

$$\mathcal{J} = -\frac{\Omega}{4} \int |z|^2 \hat{k} |z|^2 du, \quad (5.9)$$

and after variation with respect to \bar{z} we find that the conformal map satisfies:

$$\Omega^2 z \hat{k} |z|^2 + 2\sigma \partial_u \left(\frac{z_u}{|z_u|} \right) + 2i\lambda z_u = \hat{P}^+ f \quad (5.10)$$

We apply the projector, \hat{P} , to the both sides of this equation and discover that:

$$2i\lambda z_u + \Omega^2 \hat{P} \left[z \hat{k} |z|^2 \right] + 2\sigma \partial_u \hat{P} \left[\frac{z_u}{|z_u|} \right] = 0 \quad (5.11)$$

and λ is the same as the Bernoulli constant, β .

6. Linear Waves

We will now investigate small amplitude travelling waves considering the conformal map z in the form:

$$z(u, t) = z_0 + \frac{i}{k_0} e^{-iu} (1 + \delta z(u, t)), \quad (6.1)$$

$$\Phi(u, t) = -\beta t + \delta \Phi(u, t), \quad (6.2)$$

where $\delta z(u, t)$ and $\delta \Phi(u, t)$ are small. We write the kinematic equation (4.6) while keeping only the terms linear in δz , and $\delta \Phi$ which yields:

$$\frac{i}{k_0^2} (\partial_t \delta z + \partial_t \delta \bar{z}) = \delta \bar{\Phi}_u - \delta \Phi_u. \quad (6.3)$$

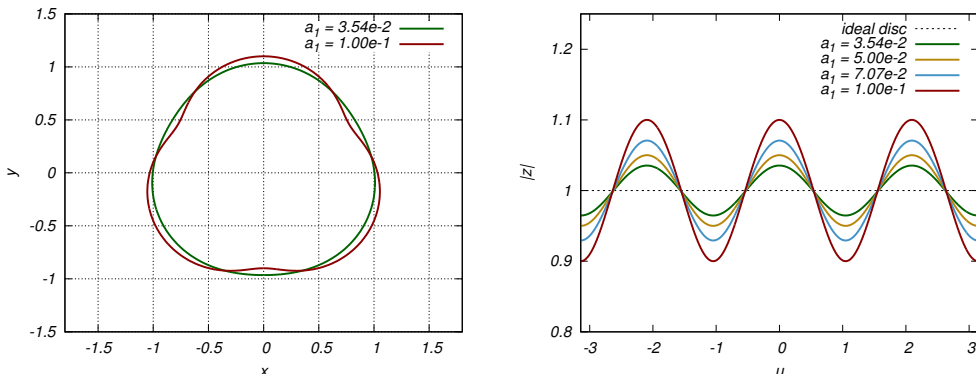


FIGURE 1. (Left) The shape of a perturbed droplet with $k = 3$, $k_0 = 1$, and $a_1 = 3.54 \times 10^{-2}$ (green), and $a_1 = 0.1$ (red) in the formula (6.10). (Right) The $|z(u, t = 0)|$ as a function of conformal variable u for ideal disc (black dotted line), and four values of amplitude a_1 . These conformal maps are the initial data for a sequence of numerical simulations to demonstrate linear standing and traveling waves.

By applying the projection operator to the linearized equation, we find that:

$$\partial_t \delta z = ik_0^2 \partial_u \delta \Phi, \quad (6.4)$$

and by substituting (6.1)–(6.2) in the dynamic equation (4.22) and keeping only the terms of leading order we find:

$$-\beta + \sigma k_0 + \delta \Phi_t - \sigma k_0 (\partial_u^2 + 1) \delta z = 0. \quad (6.5)$$

We find that $\beta = \sigma k_0$, and find the linearization system:

$$\frac{\partial}{\partial t} \begin{pmatrix} \delta \Phi \\ \delta z \end{pmatrix} = \begin{pmatrix} 0 & \sigma k_0 (1 + \partial_u^2) \\ ik_0^2 \partial_u & 0 \end{pmatrix} \begin{pmatrix} \delta \Phi \\ \delta z \end{pmatrix} \quad (6.6)$$

When $k > 1$ the eigenfunctions of the linearization matrix can be written in the form:

$$\delta \Phi, \delta z \sim e^{-i(ku - \omega t)}, \quad (6.7)$$

and the dispersion relation of linear waves is given by:

$$\omega^2 = \sigma k_0^3 k [k^2 - 1], \quad (6.8)$$

The admissible perturbations are integers, and thus $\omega^2(k)$ is non-negative, the general form of a linear perturbation is given by:

$$\Phi(u, t) = -\sigma k_0 t + \frac{i\omega}{k_0^2 k} \left[a_1 e^{-i(ku - \omega t)} - a_2 e^{-i(ku + \omega t)} \right], \quad (6.9)$$

$$z(u, t) = \frac{i}{k_0} e^{-iu} \left[1 + a_1 e^{-i(ku - \omega t)} + a_2 e^{-i(ku + \omega t)} \right], \quad (6.10)$$

and the perturbed conformal map satisfies both $z(w \rightarrow -i\infty, t) = 0$ and (3.11). The constants a_1, a_2 are free. By setting one of the constants to zero we find a linear traveling wave, and by setting $a_1 = a_2$ we find a linear standing wave solution. The standing wave does not result in rotation of the surface of the droplet, however in a traveling wave the surface shape rotates with the angular velocity, Ω , in the $z = x + iy$ plane. The angular velocity, Ω , is determined from (5.1) and is given by:

$$\Omega^2 = \frac{\omega^2}{k^2} = \sigma k_0^3 \left(k - \frac{1}{k} \right). \quad (6.11)$$

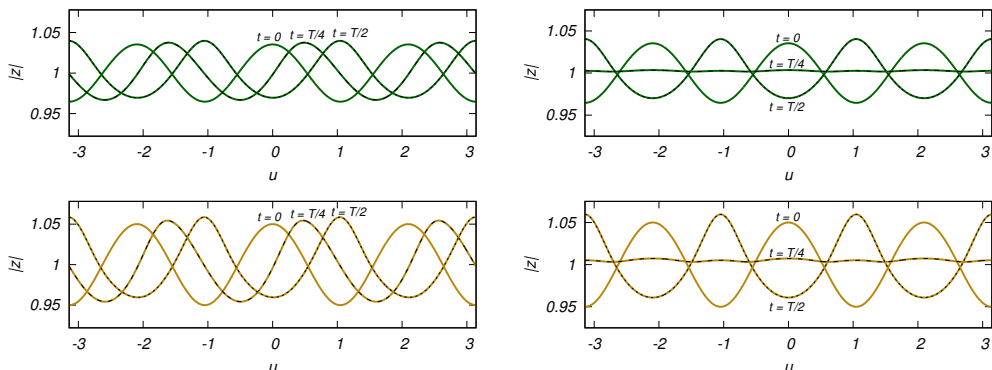


FIGURE 2. The magnitude of the conformal map $|z(u, t)|$ for a traveling wave (left) of small amplitude $a_1 = 0.025\sqrt{2}$ (left top), and amplitude $a_1 = 0.05$ (left bottom); and the magnitude of the conformal map $|z(u, t)|$ for a standing wave (right) of small amplitude $a_1 = a_2 = 0.0125\sqrt{2}$ (right top) and $a_1 = a_2 = 0.025$ (right bottom).

For the conformal wavenumber $k = 1$, the frequency ω vanishes, and there is no wave motion. The eigenfunction of the linearization matrix is sought in the form:

$$\delta z = A(t)e^{-iu} \quad \text{and} \quad \delta \Phi = B(t)e^{-iu}. \quad (6.12)$$

The linearization matrix is singular with a 2×2 Jordan block and zero eigenvalue:

$$\frac{d}{dt} \begin{pmatrix} A \\ B \end{pmatrix} = \begin{pmatrix} 0 & k_0^2 \\ 0 & 0 \end{pmatrix} \begin{pmatrix} A \\ B \end{pmatrix} \quad (6.13)$$

and the general solution is given by:

$$A(t) = (c_1 k_0^2 t + c_2) \quad \text{and} \quad B(t) = c_1 \quad (6.14)$$

where c_1 and c_2 are free constants. By the equations (6.1) and (3.2),(3.11), we find that the conformal map becomes:

$$z(u, t) = \frac{i}{k_0} [-\bar{A} + e^{-iu} + A e^{-2iu}] + O(g^2), \quad (6.15)$$

we note that a conformal remapping of the stationary disc (4.9) with a time-dependent parameter A coincides up to quadratic terms in A with the generalized eigenfunction for the zero eigenvalue:

$$z(u, t) = \frac{i e^{-iu}}{k_0} \frac{1 - \bar{A} e^{iu}}{1 - A e^{-iu}} = \frac{i}{k_0} [-\bar{A} + e^{-iu} + A e^{-2iu}] + O(A^2) \quad (6.16)$$

This is no coincidence, because variation of the function $A(t)$ does not lead to a change in the shape of the surface of the disc in the physical plane, but only moves the image of the point at $w \rightarrow -i\infty$ to $-i\bar{A}/k_0$.

The kinetic energy of a linear wave can be computed exactly and is given by the formula:

$$\mathcal{K} = \frac{\sigma\pi}{2k_0} (k^2 - 1) |a_1|^2, \quad (6.17)$$

and the potential energy may be computed approximately up to the terms of the order

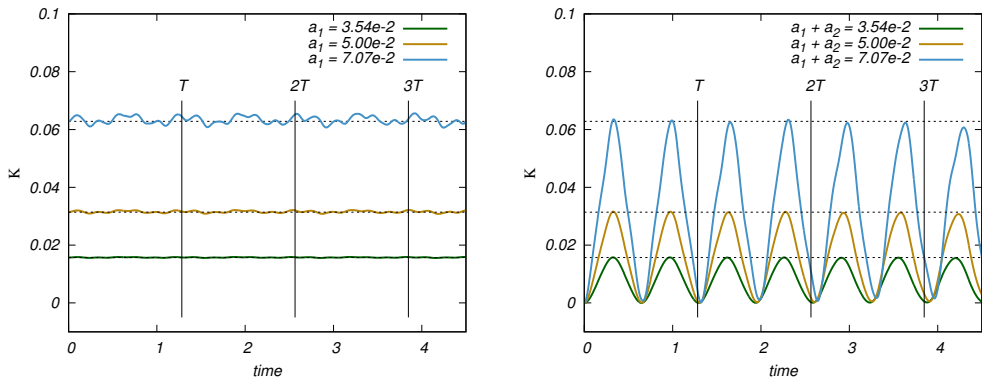


FIGURE 3. The kinetic energy as a function of time in five simulations with $k = 3$, and various values of amplitude: $0.025\sqrt{2}$ (green), $a = 0.05$ (gold), $a = 0.05\sqrt{2}$ (blue). (Left) The kinetic energy of a true linear traveling waves is constant, however since the amplitude is small but finite, we see small amplitude beats coming from nonlinear coupling of Fourier modes. The larger the amplitude is the stronger are the deviations from constant given by the equation (6.17). (Right) The kinetic energy of a true standing wave is at double the frequency of the oscillations of the surface, yet because the amplitude is small but finite some nonlinear corrections are present. The vertical lines at $t = T$, $t = 2T$ and $t = 3T$ mark the ends of the first, second and third period of linear wave. As evident from the figure, the frequency decreases due to a nonlinear frequency shift, especially evident for the largest amplitude wave (blue).

$|a_1|^2$, and is given by:

$$\mathcal{P} = \frac{2\pi\sigma}{k_0} + \frac{\sigma\pi}{2k_0} (k+1)^2 |a_1|^2. \quad (6.18)$$

7. Numerical Simulation

We solve the equations (4.26)–(4.27) numerically using a pseudospectral method to approximate the functions R and V . The projection operator and derivatives with respect to u -variable are applied as a Fourier multipliers. The Runge–Kutta method of fourth order is used for time integration.

We illustrate linear waves by solving the time-dependent equations with the initial data given by the equations (6.10)–(6.9). In the simulations of traveling waves (see the left panels of Fig. 2 and Fig. 3) the amplitude $a_2 = 0$, and

$$a_1 = 0.025\sqrt{2}, 0.05, \text{ and } a_1 = 0.05\sqrt{2}. \quad (7.1)$$

In the simulations of standing waves (see the right panel of Fig. 2 and Fig. 3) the amplitudes a_1 and a_2 are equal in the equations (6.10)–(6.9) and are:

$$a_1 = 0.0125\sqrt{2}, 0.025, \text{ and } a_1 = 0.025\sqrt{2}. \quad (7.2)$$

The accuracy of simulations is controlled by measuring the total energy and mass in the course of the simulation, as well as ensuring that the Fourier spectrum of R and V is resolved to machine precision.

8. Conclusion

Breaking of water waves in deep ocean is associated with generation of water droplet spray. The water spray partially accounts for the energy–momentum transfer in wave turbulence. The physical processes that generate water spray have been observed in physical

ocean (see reference Erinin *et al.* (2019)), as well as theoretically Dyachenko & Newell (2016). As a plunging breaker develops on the crest of an ocean wave there is an abrupt growth of small scale features, and several physical mechanisms suddenly come into play. The force of surface tension that normally has little effect on long gravity waves, becomes one of the dominant forces at the crest of breaking wave. The detachment of a water droplet from a plunging breaker is a complicated and nonlinear process, and the present work does not make an attempt to understand it to the full extent.

We considered a problem of deformation of a fluid disc with a free boundary subject to the force of surface tension. We derived that a conformal map associated with such a flow satisfies a pseudodifferential equation that is similar to Babenko equation for the Stokes wave. We have shown that the motion of small amplitude deformations is subject to the linear dispersion relation given by (6.8). We demonstrate the results of numerical simulation with initial data close to linear waves, and observe excellent agreement for small amplitude waves, and report significant deviations as amplitude grows.

The nonlinear equation (5.3), or its complex form (5.4), can be efficiently solved by the standard method that are applicable to the Stokes wave problem, e.g. the generalized Petviashvili method, or the Newton-Conjugate-Gradient to obtain nonlinear solutions. The present work is a precursor to further investigation of nonlinear waves, and of special interest is the nature of the limiting wave. Of particular interest is the question of the existence of the limiting wave, and its nature and singularities. One may speculate that the limiting wave will not form an angle on the surface, since it would make the potential energy very large; yet higher order, curvature singularity may form on the surface. The construction of nonlinear waves is the subject of ongoing work.

9. Acknowledgements

The author would like to thank Alexander I. Dyachenko for fruitful discussion. The present work was supported by NSF grant DMS-1716822. The author would like to thank the developers and maintainers of FFTW library Frigo & Johnson (2005) and the entire GNU project.

REFERENCES

- BABENKO, K. I. 1987 Some remarks on the theory of surface waves of finite amplitude. *Soviet Math. Doklady* **35**, 599–603.
- CRAPPER, G. D. 1957 An exact solution for progressive capillary waves of arbitrary amplitude. *Journal of Fluid Mechanics* **2**, 532–540.
- CROWDY, D. G. 1999a Circulation-induced shape deformations of drops and bubbles: Exact two-dimensional models. *Physics of Fluids* **11** (10), 2836–2845.
- CROWDY, D. G. 1999b Exact solutions for steady capillary waves on a fluid annulus. *Journal of Nonlinear Science* **9** (6), 615–640.
- DIRICHLET, G. L. 1860 Untersuchungen über ein Problem der Hydrodynamik. *Abh. Kön. Gest. Wiss. Göttingen* **8**, 3–42.
- DYACHENKO, A. I. 2001 On the dynamics of an ideal fluid with a free surface. *Dokl. Math.* **63**, 115–117.
- DYACHENKO, A.I., KUZNETSOV, E.A., SPECTOR, M.D. & ZAKHAROV, V.E. 1996a Analytical description of the free surface dynamics of an ideal fluid (canonical formalism and conformal mapping). *Physics Letters A* **221** (1), 73 – 79.
- DYACHENKO, A. I., ZAKHAROV, V. E. & KUZNETSOV, E. A. 1996b Nonlinear dynamics of the free surface of an ideal fluid. *Plasma Physics Reports* **22** (10), 829–840.
- DYACHENKO, A. I., DYACHENKO, S. A., LUSHNIKOV, P. M. & ZAKHAROV, V. E. 2019 Dynamics

- of poles in two-dimensional hydrodynamics with free surface: new constants of motion. *Journal of Fluid Mechanics* **874**, 891–925.
- DYACHENKO, S. & NEWELL, A. C. 2016 Whitecapping. *Studies in Applied Mathematics* **137** (2), 199–213.
- DYACHENKO, SERGEY A. 2019 On the dynamics of a free surface of an ideal fluid in a bounded domain in the presence of surface tension. *Journal of Fluid Mechanics* **860**, 408418.
- ERININ, M. A., WANG, S. D., LIU, R., TOWLE, D., LIU, X. & DUNCAN, J. H. 2019 Spray generation by a plunging breaker. *Geophysical Research Letters* **46** (14), 8244–8251.
- FRIGO, M. & JOHNSON, S. G. 2005 The design and implementation of fftw3. *Proceedings of the IEEE* **93** (2), 216–231.
- KINNERSLEY, W. 1976 Exact large amplitude capillary waves on sheets of fluid. *J. Fluid Mech.* **77**, 229–241.
- LANDAU, L. D. & LIFSHITZ, E. M. 1976 *Mechanics*, , vol. 1. Butterworth–Heinemann.
- STOKES, G. G. 1880 *Mathematical and Physical Papers*, , vol. 1. Cambridge University Press.
- ZAKHAROV, V. E. 1968 Stability of periodic waves of finite amplitude on the surface of a deep fluid. *Journal of Applied Mechanics and Technical Physics* **9** (2), 190–194.